Modelling of a Vector-current Controlled UPFC and Comprehensive Comparison with the Power-angle Control Strategy

Bixing Ren[1,a], Wenjuan Du[1], Hui Cai[2], Haifeng Wang[1], Xiangfeng Wang[1] and Jianpeng Zhang[1]

[1]North China Electric Power University, Beijing, 102206, China
[2]State Grid Jiangsu Economic Research Institute, Nanjing, 210008, China

[a] Corresponding author : renbixing@126.com

Abstract. This paper establishes the non-linear dynamic mathematical model of the vector-current controlled unified power flow controller (UPFC) and the linearized model of the UPFC is derived in detail afterwards for the analysis of dynamic performance stability. Then, the paper carries out deep investigations on the comparison and analysis for the above two control strategies applied to the UPFC in the aspects of dynamic interaction and auxiliary damping effect. The relative gain array (RGA) method is used to assess the dynamic interactions among the multiple control functions of the UPFC, and damping torque analysis (DTA) method is used to compare the damping performance of the UPFC auxiliary damping controller. The results of quantitative comparison by RGA and DTA analysis show that the vector-current controlled UPFC exhibits better decoupling characteristic among multiple control loops, while the power-angle controlled UPFC exhibits better auxiliary damping performance. Conclusions are further validated by the non-linear simulation results via a two-area four-machine system.

1 Introduction

Vector-current control and power-angle control are the two typical control strategies of voltage source converter (VSC) that have been mostly investigated. The UPFC, consisting of two VSCs, is a multiple-functional FACTS controller which has the primary duty to control the power flow while has secondary functions of voltage regulation and oscillation damping etc. [1-2]. For small signal stability analysis, such as electromechanical oscillation and dynamic interaction, published researches have mainly focused on power-angle controlled UPFC [3-5]. Vector-current control strategy is adopted in the UPFC in China [6] and there is a potential risk of dynamic interactions among the UPFC, which may bring negative effects to the UPFC control and operation.

This paper establishes the non-linear dynamic mathematical model of the vector-current controlled UPFC and the linearized model of the UPFC is derived afterwards. Then, the paper carries out comprehensive comparisons between the above two control strategies adopted to the UPFC. Based on the derived model, dynamic interactions among the multiple control functions of the UPFC are investigated by use of the method of the relative gain array (RGA) [7-9]. Besides, damping torque analysis (DTA) method [10-12] is used to compare the auxiliary damping performance of the UPFC. Conclusions of the comparison and analysis are further validated by the non-linear simulation.

2 Dynamic mathematical model and control strategy

2.1 Non-linear model and linearized model of the vector-current controlled UPFC

Without loss of generality, a UPFC is assumed to be installed in a multi-machine power system between node 1 and node 2. The UPFC consists of an excitation transformer (ET), a boosting transformer (BT), two VSCs and a DC link capacitor, which are shown in Figure 1.

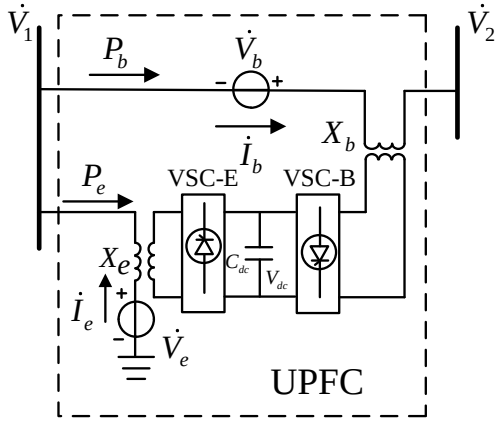

Figure1. The multi-machine power system with UPFC installed

The non-linear dynamic equations of the vector-current controlled UPFC can be derived as follows:

$$\begin{cases} \dfrac{d}{dt}(\dfrac{1}{2}C_{dc}V_{dc}^2) = C_{dc}V_{dc}\dfrac{dV_{dc}}{dt} = -(P_e + P_b) = -(V_{ed}I_{ed} + V_{eq}I_{eq} + V_{bd}I_{bd} + V_{bq}I_{bq}) \\ \dfrac{dI_{ex}}{dt} = \omega_0\left[\dfrac{1}{X_e}(V_{ex} - V_{1x}) + I_{ey}\right], \dfrac{dI_{ey}}{dt} = \omega_0\left[\dfrac{1}{X_e}(V_{ey} - V_{1y}) - I_{ex}\right] \\ \dfrac{dI_{bx}}{dt} = \omega_0\left[\dfrac{(V_{1x} - V_{2x}) + V_{bx}}{X_b} + I_{by}\right], \dfrac{dI_{by}}{dt} = \omega_0\left[\dfrac{(V_{1y} - V_{2y}) + V_{by}}{X_b} - I_{bx}\right] \end{cases} \quad (1)$$

By taking the direction of $\dot{V}_1$ in Figure 2 as the d axis reference direction of the d-q coordinate system of the UPFC, the transformation equation of the vector $\dot{F}$ between d-q coordinate system and x-y coordinate system can be can be expressed in the equation (2).

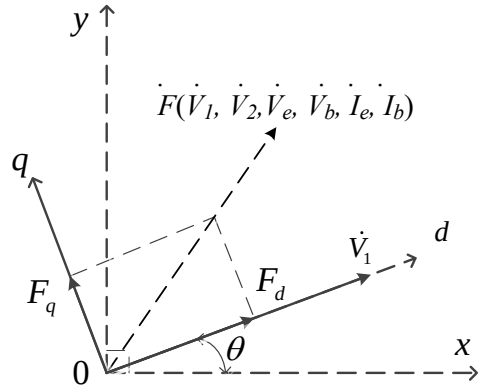

Figure2. Coordinate transformation relation

$$\begin{bmatrix} F_d \\ F_d \end{bmatrix} = \begin{bmatrix} \cos\theta & \sin\theta \\ -\sin\theta & \cos\theta \end{bmatrix} \begin{bmatrix} F_x \\ F_y \end{bmatrix} \quad (2)$$

Substituting the linearized form of equation (2) into equation (1), the following equation can be obtained.

$$\begin{cases} \dfrac{d\Delta V_{dc}}{dt} = upfc\_a_1\Delta V_{dc} + upfc\_a_2\Delta I_{ex} + upfc\_a_3\Delta I_{ey} + upfc\_a_4\Delta I_{bx} + upfc\_a_5\Delta I_{by} + \\ upfc\_a_6\Delta V_{1x} + upfc\_a_7\Delta V_{1y} + upfc\_a_8\Delta V_{ed} + upfc\_a_9\Delta V_{eq} + upfc\_a_{10}\Delta V_{bd} + upfc\_a_{11}\Delta V_{bq} \\ \dfrac{d\Delta I_{ex}}{dt} = upfc\_b_1\Delta I_{ey} + upfc\_b_2\Delta V_{1x} + upfc\_b_3\Delta V_{1y} + upfc\_b_4\Delta V_{ed} + upfc\_b_5\Delta V_{eq} \\ \dfrac{d\Delta I_{ey}}{dt} = upfc\_c_1\Delta I_{ex} + upfc\_c_2\Delta V_{1x} + upfc\_c_3\Delta V_{1y} + upfc\_c_4\Delta V_{ed} + upfc\_c_5\Delta V_{eq} \\ \dfrac{d\Delta I_{bx}}{dt} = upfc\_d_1\Delta I_{by} + upfc\_d_2\Delta V_{1x} + upfc\_d_3\Delta V_{1y} + upfc\_d_4\Delta V_{2x} + upfc\_d_5\Delta V_{2y} + upfc\_d_6\Delta V_{bd} + upfc\_d_7\Delta V_{bq} \\ \dfrac{d\Delta I_{by}}{dt} = upfc\_e_1\Delta I_{bx} + upfc\_e_2\Delta V_{1x} + upfc\_e_3\Delta V_{1y} + upfc\_e_4\Delta V_{2x} + upfc\_e_5\Delta V_{2y} + upfc\_e_6\Delta V_{bd} + upfc\_e_7\Delta V_{bq} \end{cases} \tag{3}$$

2.2 Principle of vector-current control strategy

The series part of the UPFC can control the active and reactive power flow on the transmission line while the shunt part of the UPFC can regulate the voltage of the connecting node. Thus, the principle of the vector-current control strategy of the UPFC is shown in Figure 3.

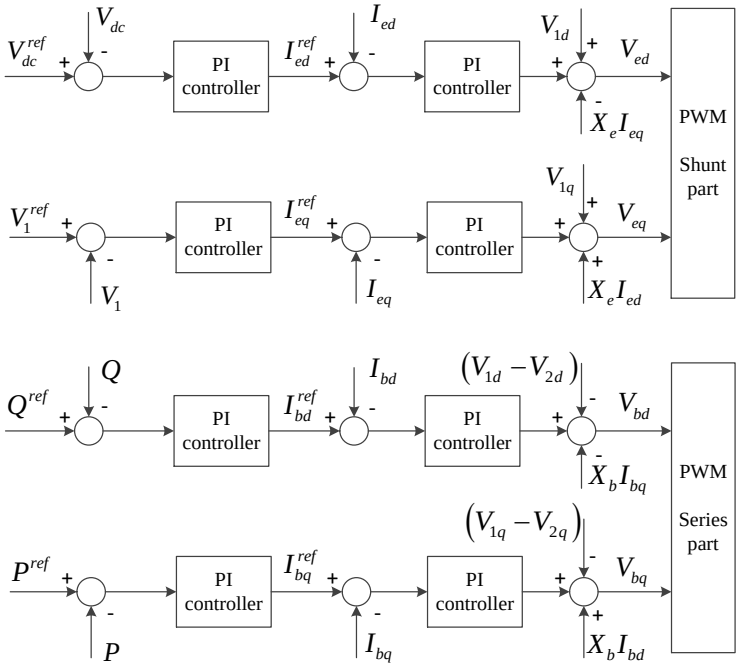

Figure3. Control strategy of vector-controlled UPFC

3 Two Quantitative comparison methods

3.1 Dynamic interaction analysis of UPFC controllers based on RGA method

A relative gain λ_{ij} for an input–output control pair $y_i - u_j$ is defined as the ratio between the un-controlled gain and controlled gain [7]. If there exists an element λ_{ij} in RGA is close to 1, it can be concluded that the interactions are relatively weak; otherwise the interactions are relatively strong.

$$\lambda_{ij} = \frac{\partial y_i / \partial u_j \,|(\text{all loops off})}{\partial y_i / \partial u_j \,|(\text{all loops but } y_i - u_j \text{ perfect})} \tag{4}$$

The linearized differential equations of the multi-machine power system with a UPFC installed can be written as:

$$\begin{cases} \Delta \dot{\boldsymbol{X}} = \boldsymbol{A}\Delta\boldsymbol{X} + \boldsymbol{B}\Delta\boldsymbol{U} \\ \Delta \boldsymbol{Y} = \boldsymbol{C}\Delta\boldsymbol{X} + \boldsymbol{D}\Delta\boldsymbol{U} \end{cases} \tag{5}$$

where $\Delta\boldsymbol{X}$ is the vector of state variables, including generators and UPFC; $\Delta\boldsymbol{U}$ is the vector of control variables; $\Delta\boldsymbol{Y}$ is the vector of eliminate algebra variable.

By transforming equation (5) into frequency domain, transfer functions equation (6) can be gained.

$$\boldsymbol{G}(s) = \boldsymbol{Y}(s)/\boldsymbol{U}(s) = [\boldsymbol{C}(s\boldsymbol{I} - \boldsymbol{A})^{-1}\boldsymbol{B} + \boldsymbol{D}] \tag{6}$$

RGA can be calculated by using equation (7) in a square array

$$\boldsymbol{R}_{\mathrm{RGA}}(\boldsymbol{G}(0)) = \boldsymbol{G}(0) \otimes (\boldsymbol{G}(0)^{-1})^{T} \tag{7}$$

where symbol $\otimes$ is product of corresponding elements in two arrays under steady state, $\boldsymbol{G}(0)$ is the steady state value of the corresponding transfer function array $\boldsymbol{G}(s)$.

The simplified introduction of the power-angle controlled UPFC is shown in [3-5], The RGA matrixes are shown as follows

$$RGA = \begin{array}{c} \\ \Delta V \\ \Delta V_{dc} \\ \Delta Q \\ \Delta P \end{array} \begin{array}{c} \begin{array}{cccc} \Delta V_{\mathrm{eq}} & \Delta V_{\mathrm{ed}} & \Delta V_{\mathrm{bd}} & \Delta V_{\mathrm{bq}} \end{array} \\ \begin{bmatrix} \lambda_{11} & \lambda_{12} & \lambda_{13} & \lambda_{14} \\ \lambda_{21} & \lambda_{22} & \lambda_{23} & \lambda_{24} \\ \lambda_{31} & \lambda_{32} & \lambda_{33} & \lambda_{34} \\ \lambda_{41} & \lambda_{42} & \lambda_{43} & \lambda_{44} \end{bmatrix} \end{array}, \quad RGA = \begin{array}{c} \\ \Delta V \\ \Delta V_{dc} \\ \Delta Q \\ \Delta P \end{array} \begin{array}{c} \begin{array}{cccc} \Delta m_E & \Delta \delta_E & \Delta m_B & \Delta \delta_B \end{array} \\ \begin{bmatrix} \lambda_{11} & \lambda_{12} & \lambda_{13} & \lambda_{14} \\ \lambda_{21} & \lambda_{22} & \lambda_{23} & \lambda_{24} \\ \lambda_{31} & \lambda_{32} & \lambda_{33} & \lambda_{34} \\ \lambda_{41} & \lambda_{42} & \lambda_{43} & \lambda_{44} \end{bmatrix} \end{array} \tag{8}$$

$$(vector - current\ control) \qquad (phase - angle\ control)$$

3.2 Auxiliary damping analysis of UPFC stabilizers based on DTA method

Auxiliary damping controllers are superposed upon the main control loops so as to damp low frequency oscillation. Without loss of generality, A UPFC with one auxiliary damping controller is shown in Figure 4.

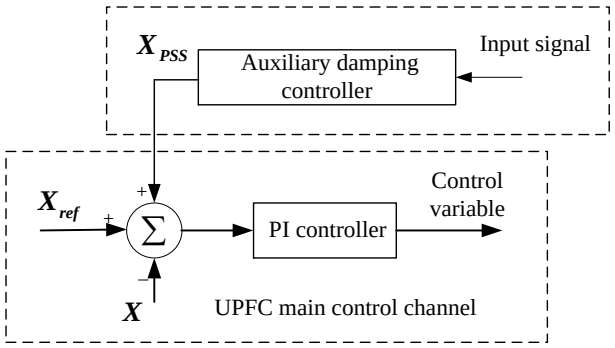

Figure4. Block diagram of auxiliary damping controller equipped on UPFC

When PI controllers of the UPFC are put into service and auxiliary damping signals are imported, the linearized equations of the system can be written as:

$$\dot{\boldsymbol{X}} = \boldsymbol{A}\Delta\boldsymbol{X} + \boldsymbol{E}\Delta\boldsymbol{S} \tag{9}$$

where $\Delta\boldsymbol{X}$ is the vector of state variables including generators and the UPFC, $\Delta\boldsymbol{S}$ is the additional input signal of the UPFC.

According to DTA theory [10-12], for the i^{th} oscillation mode λ_i, the damping torque provided by the damping controller $G(s)$ to the electromechanical oscillation loop of j^{th} generator is:

$$\Delta T_{ij} = \mathrm{Re}[F_j(\lambda_i)\sigma_j(\lambda_i)G(\lambda_i)]\Delta\omega_j = \mathrm{Re}[H_{ij}\angle\varphi_{ij}G(\lambda_i)]\Delta\omega_j = D_{ij}\Delta\omega_j,\ j=1, 2, \cdots, N \tag{10}$$

where D_{ij} is the damping torque coefficient; ω_j is the angular velocity of the j^{th} generator; F_j is the forward channel transfer function from ΔS to the electromechanical oscillation loop of the j^{th} generator.

Define the DTA index as:

$$|\mathrm{DTA}| = \frac{\Delta\lambda_i}{\Delta G(\lambda_i)} = \left|\sum_{j=1}^{N} S_{ij}H_{ij}\angle\varphi_{ij}\right| \tag{11}$$

where S_{ij} is the sensitivity coefficient[12].

The index is the sensitivity of oscillation mode λ_i to the additional damping controller $G(s)$ and it can be used for assessing the auxiliary damping effect of UPFC stabilizers under two control strategies.

4 Simulation results

In order to effectively distinguish the dynamic interactions and auxiliary damping effects between the two kinds of control strategies, a two-area four-machine system is used in the paper, shown in Figure 5, and the system parameters are listed in [13]. The UPFC is installed in the transmission line between bus12 and bus13, and its initial per-unit values are: $P_t = 2.0$, $Q_t = 0.2$, $V_{dc} = V_1 = 1$.

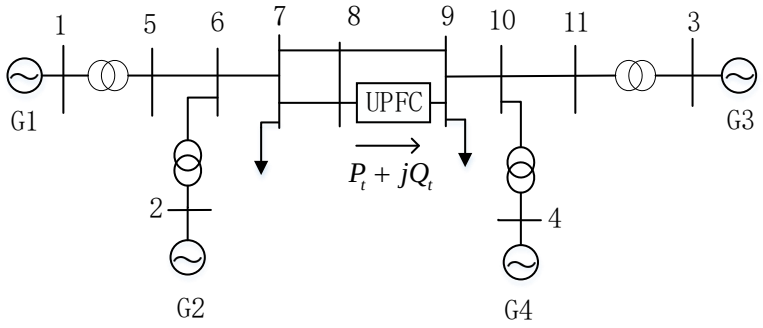

Figure 5. Four-machine power system with a UPFC

4.1 Dynamic interaction comparison and analysis

The calculation results of RGA array are shown in Table 1.As shown in Table 1, secondary diagonal elements λ_{12} and λ_{21} of RGA with different control strategy are close to 1. By the interaction analysis on SVG [9], if secondary diagonal elements of RGA are close to 1, it can be concluded that multiple control functions are well performed. Thus, interaction between the shunt controllers of the UPFC which can be regarded as a SVG is weak. Meanwhile, from Table 1 it can also be noted that diagonal elements λ_{33} and λ_{44} of RGA with vector-current control strategy are close to 1, but the ones with power-angle control strategy are greater negative. Thus, it can be concluded that dynamic interaction between the series controllers of the UPFC under vector-current control is weak, while the ones under power-angle control is strong.

Table 1. RGA array corresponding to different control strategy

Control strategy	Vector-current control	Power-angle control

RGA array	$\begin{bmatrix} -0.2399 & 0.9180 & 0.0069 & 0.3150 \\ 0.9345 & -0.1226 & 0.1717 & 0.0163 \\ 0.1349 & 0.1005 & 0.7338 & 0.0308 \\ 0.1705 & 0.1041 & 0.0876 & 0.6378 \end{bmatrix}$	$\begin{bmatrix} 0.0199 & 9.9469 & 1.2767 & -10.2435 \\ 0.9477 & 0.0000 & 0.0533 & 0.0000 \\ 0.0215 & 0.1239 & -24.7234 & 25.5779 \\ 0.0138 & -9.0708 & 24.3914 & -14.3444 \end{bmatrix}$

Figure 6 shows the results of step response of the multiple controllers equipped in the UPFC. In the simulation, the reference value of parallel bus voltage increases by 2% at 1.0s. The simulation curve of the vector-current controlled UPFC recovers to the steady state in a shorter time than the power-angle controlled UPFC, which means that the structure of inner-current loop is helpful to system dynamic stability. However, the amplitudes of UPFC series control loops under power-angle control oscillate heavily. So it can be concluded that the vector-current controlled UPFC exhibits better decoupling performance among multiple control loops than the power-angle controlled UPFC, which validates the analysis of RGA shown in Table 1.

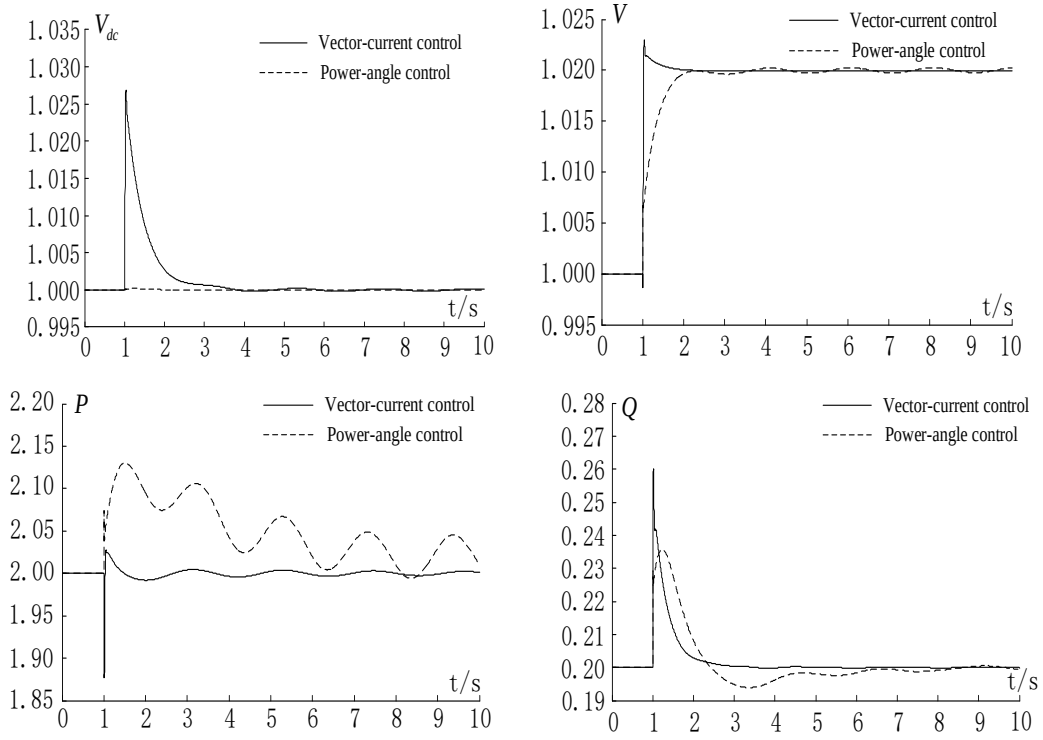

Figure 6. Step response of the UPFC

4.2 Auxiliary damping effects comparison and analysis

The four-machine system has an inter-area oscillation with weak damping mode $\lambda = -0.06 + j2.92$, which is chosen for DTA analysis. The calculation results of DTA index are shown in Table 2.

Table 2. DTA index corresponding to different control strategy

Control strategy	Auxiliary controller channel	DTA index
Power-angle control	$m_e - V$	7.421
	$\delta_e - V_{dc}$	6.427
	$m_b - Q$	3.805
	$\delta_b - P$	0.152
Vector-current control	$V_{bd} - Q$	3.125

	$V_{bq}-P$	2.953
	$V_{eq}-V$	2.437
	$V_{ed}-V_{dc}$	1.474

From Table 2 it can be seen that the DTA magnitude of auxiliary controller channel under power-angle control is more than that under vector-current control except for $\delta_b - P$ channel.

Figure 7 shows the non-linear simulations of the auxiliary damping effects of UPFC with two control strategies respectively. Without auxiliary damping controllers, the swing amplitude curve of generator angle difference shown in Fig.7(a) is less than that shown in Fig.7(b), it can be understood that the structure of inner-current loop of vector-current controlled UPFC improves system stability. However, it can be also seen that the power-angle controlled UPFC has much more auxiliary damping effects on the oscillation mode than the vector-current controlled UPFC, which verifies the correctness of the DTA analysis.

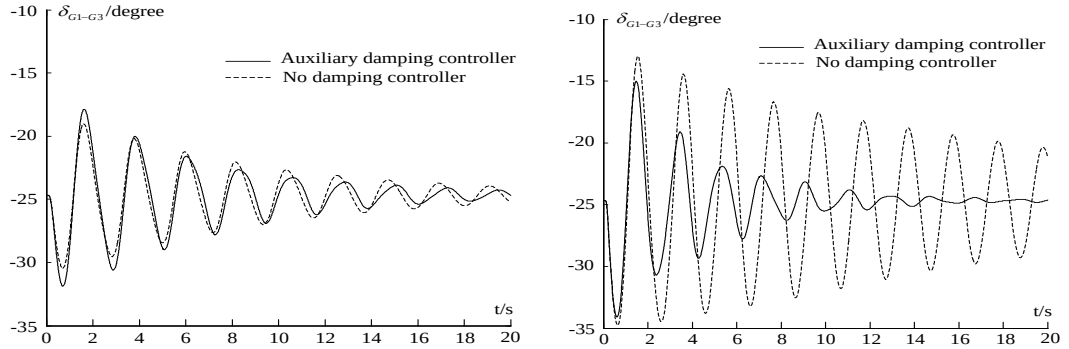

7(a) vector-current control strategy 7(b) power-angle control strategy

Figure 7. Generator angle difference

5 Conclusion

This paper establishes the non-linear dynamic model of the vector-current controlled UPFC and the linearized model of the UPFC is derived afterwards. Based on the derived linearized model, the comprehensive comparisons, dynamic interaction and auxiliary damping effect, between the vector-current control strategy and power-angle control strategy are carried out by the RGA and the DTA method respectively. Conclusions are listed as follows:

(1) For the dynamic interaction, the vector-current controlled UPFC exhibits better decoupling characteristic among multiple controllers than the power-angle controlled UPFC.

(2) For the auxiliary damping effect, the power-angle controlled UPFC exhibits better auxiliary damping performance on the damping of electromechanical oscillation modes than the vector-current controlled UPFC.

6 Acknowledgment

The work is supported by the Fundamental Research Funds for the Central Universities (2016XS09), state grid of cooperation of China (project SGJS0000FZJS1501126).

References

[1] J. Svensson. “Grid-connected voltage source converter”, Ph.D. dissertation, Chalmers Univ. Technol., Gothenburg, Sweden, (1998).

[2] H.F.Wang. “Damping function of unified power flow controller”, IEE Proceedings- Generation, Transmission and Distribution, vol. 146, no. 3, pp. 81-87, (1999).

[3] H.F.Wang. “A unified model for the analysis of FACTS devices in damping power system oscillations-Part III: Unified Power Flow Controller”, IEEE Trans on power delivery, vol. 15, no. 3, pp. 978-983, (2000).

[4] H.F.Wang. "Interactions and multivariable design of multiple control functions of a unified power flow controller", International Journal of Electrical Power & Energy Systems, vol. 24, no. 7, pp. 591-600, (2002).
[5] DU Wen-juan, WANG Hai-feng, M Jazaeri, et al. "Effect of Variations of Control Operating Point of UPFC on Power System Stability and Control Performance", Automation of Electric Power Systems, vol. 29, no. 20, pp. 40-45, (2005).
[6] QI Wanchun, YANG Lin, SONG Pengcheng, et al. "UPFC System Control Strategy Research in Nanjing Western Power Grid", Power System Technology, vol. 40, no. 1, pp. 92-96, (2016).
[7] Bristol E H. "On a New measure of Interaction for Multivariable Process control", IEEE Transactions on Automatic Control, vol. 11, no. 1, pp. 133-134, (1966).
[8] Zhang, L, Zhang P.X, Wang H.F et al. "Interaction assessment of FACTS control by RGA for the effective design of FACTS damping controllers", Generation, Transmission and Distribution, IEE Proceedings, vol. 153, no. 5, pp. 610-616, (2006).
[9] JIANG Quan-yuan, ZOU Zhen-yu, WU Hao et al. "Interaction Analysis of FACTS Controllers Based on RGA Principle", Proceedings of the CSEE, vol. 25, no. 11, pp. 24-28, (2005).
[10] Swift F J, WANG H F. "The connection between modal analysis and eletric torque analysis in studying the oscillation stability of multi-machine power systems", Electrical Power and Energy Systems, vol. 19, no. 5, pp. 321-330, (1997).
[11] CHEN Zhong, DU Wen-juan, WANG Hai-feng, et al. "Power system low-frequency oscillations suppression with energy storage system based on DTA", Automation of Electric Power Systems, vol. 33, no. 12, pp. 8-11, (2009).
[12] CHEN Zhong. "Study of the DTA application in large scale inter-connected power system", Power System Protection and Control, vol. 39, no. 12, pp. 102-105, (2011).
[13] P. M. Anderson and A. A. Fouad. "Power System Control and Stability", New York: Wiley, (2005).